

See discussions, stats, and author profiles for this publication at: <https://www.researchgate.net/publication/49743998>

Excitation Wavelength and Fluence Dependent Femtosecond Transient Absorption Studies on Electron Dynamics of Gold Nanorods

ARTICLE in THE JOURNAL OF PHYSICAL CHEMISTRY A · APRIL 2011

Impact Factor: 2.69 · DOI: 10.1021/jp108176h · Source: PubMed

CITATIONS

8

READS

98

3 AUTHORS:



Kuai Yu

Stanford University

21 PUBLICATIONS 547 CITATIONS

SEE PROFILE



Polavarapu Lakshminarayana

Ludwig-Maximilians-University of Munich

44 PUBLICATIONS 1,272 CITATIONS

SEE PROFILE



Qing-Hua Xu

National University of Singapore

129 PUBLICATIONS 3,334 CITATIONS

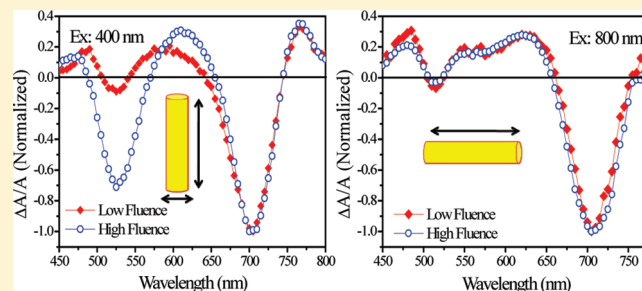
SEE PROFILE

Excitation Wavelength and Fluence Dependent Femtosecond Transient Absorption Studies on Electron Dynamics of Gold Nanorods

Kuai Yu,^{†,‡} Lakshminarayana Polavarapu,[†] and Qing-Hua Xu^{*,†,‡}

[†]Department of Chemistry and [‡]NUS Graduate School for Integrative Sciences and Engineering, National University of Singapore, Singapore 117543

ABSTRACT: The electron dynamics of gold nanorods were systematically studied by using femtosecond transient absorption experiments. Two different excitation wavelengths (400 and 800 nm) have been used as the excitation sources to selectively excite transverse and longitudinal modes. The transient absorption spectra were found to be strongly dependent on the excitation wavelength and fluence. Laser pulses of 800 nm excite the longitudinal mode directly, which cause an increase in the electronic temperatures and subsequent broadening and bleaching of both the longitudinal and transverse modes. Pulses of 400 nm excite both the transverse and longitudinal modes simultaneously. At low excitation fluences, the energy is distributed into two modes according to their steady state extinction coefficients, under which the transient spectra are similar to those under excitation at 800 nm. However, as the excitation fluence exceeds a threshold, the bleaching of the longitudinal plasmon band saturates and the input energies mainly flow to the transverse mode. As a result, the bleaching of the transverse mode increases rapidly. The electron–phonon dynamics show a strong correlation with the bleaching amplitude. We have tried to explain the results with a consistent picture: the bleaching amplitude and electron–phonon relaxation time are directly related to energy distribution into different modes, which are excitation wavelength and fluence dependent. Our studies help to clarify the seemingly inconsistent results in the previous studies by different research groups.



INTRODUCTION

Metal nanostructures such as silver and gold, display many unique optical properties due to formation of surface plasmons.^{1–6} Plasmons are the collective oscillation of conduction band electrons. It can produce highly confined and amplified local optical field and display many interesting light-matter interactions. The local surface plasmon resonance (SPR) properties of metal nanoparticles are strongly dependent on the size, shape, and surrounding dielectric medium of the nanostructures.⁷ A lot of effort has been devoted to synthesize metal nanoparticles of different geometries.^{8–12} The extinction spectrum of the metal nanoparticles can be tuned from the visible to near-infrared range.¹³ Gold nanorods are of particular interest and have been extensively investigated.^{14–18} Compared to the gold nanospheres, gold nanorods have two SPR bands: a longitudinal mode parallel to the long axis of the nanorod and a transverse mode perpendicular to it.¹⁹

Understanding electron dynamics in noble metal nanoparticles under optical excitation is important for exploring their potential applications.^{20,21} Femtosecond transient absorption and pump probe experiments are usually exploited to investigate their electron dynamics on a femtosecond time scale. In a typical pump probe experiment, the electron distribution is perturbed by a short pump pulse, and the resulting relaxation to equilibrium can be monitored by a time-delayed probe beam. The electron

dynamics in various gold nanoparticles have been extensively studied.^{22–27} The electron relaxation processes were usually theoretically described by a two-temperature model.²⁸ According to this model, laser excitation by a near-UV or visible pump pulse will cause an increase in electronic temperature, which results in broadening and bleaching of the plasmon resonance bands. The system subsequently relaxes back to the room temperature through a series of heat exchange processes. These sequential relaxation processes include electron–electron scattering, electron–phonon scattering, coherent lattice vibrations, and heat dissipation to the surroundings.^{22,23,29} Although the electron relaxation process has been widely studied, most of the work is focused on the spherical nanoparticles and under weak perturbation regime.^{24,30–32} There are very few reports on the transient absorption studies on gold nanorods, in which there are many inconsistencies in the previous results reported by different research groups.^{25,33,34} In particular, understanding the transient absorption spectroscopy and electron dynamics of different plasmon modes under a strong perturbation regime in gold nanorods have been less studied.

Special Issue: Graham R. Fleming Festschrift

Received: August 27, 2010

Revised: December 17, 2010

In this work, we systematically studied electron relaxation dynamics in pure gold nanorods using femtosecond transient absorption spectroscopy under different excitation fluences at 400 and 800 nm. As the energy of the 800 nm pump photon is less than the interband transition and the transverse mode of gold nanorods, only the longitudinal mode is directly excited. The 400 nm pulse is resonant with the interband transition. Both the transverse and longitudinal modes can be excited simultaneously by 400 nm pulses. The transient spectra and electron dynamics show very interesting excitation fluence dependence. The bleaching of both longitudinal and transverse bands was observed under excitation at both 400 and 800 nm by different mechanisms. The bleaching dynamics of the two modes show a strong correlation with their bleaching amplitude at raised electronic temperatures upon photoexcitation. We have tried to explain the observations in a consistent picture as a result of different energy redistributions into different modes under different excitation wavelengths and fluences. Our studies will help to clarify the inconsistency in the literature and provide a consistent understanding of the electron dynamics of gold nanorods.

EXPERIMENTS

Gold nanorods with longitudinal plasmon resonance band maximum at 715 nm were synthesized by using a previously reported seed-mediated growth method.¹⁰ The seed solution was first prepared by adding 25 μL of 0.1 M HAuCl_4 to 10 mL of 0.1 M CTAB solution in a plastic tube. A freshly prepared 0.6 mL of ice-cold 0.01 M NaBH_4 solution was quickly added all at once under vigorous stirring. The stirring was continued for another 2 min. The resulting brownish yellow solution was kept at room temperature for at least 2 h to be used as the seed solution. For seed-mediated growth, 2.0 mL of 0.01 M HAuCl_4 and 0.15 mL of 0.01 M AgNO_3 were added into 40 mL of 0.1 M CTAB solution and mixed by gentle shaking. Freshly prepared 0.32 mL of 0.1 M L-ascorbic acid solution, 0.8 mL of 1.0 M HCl, and 100 μL seed solution were then added into the mixture sequentially. The reaction mixture was then left undisturbed at least overnight for longitudinal overgrowth. The prepared gold nanorods were purified by centrifugation of nanorods solution with a speed of 12 000 rpm for 10 min to remove excess CTAB surfactant for two times. The resulting gold nanorods were used for various characterization and pump probe experiments.

The UV–visible extinction spectra of the sample were measured by using a Shimadzu UV 2450 spectrometer. Transmission electron micrograph (TEM) images were taken by using a JEOL 2010 electron microscope. The time-resolved transient absorption and pump probe experiments were performed by using a Spectra Physics Ti:sapphire oscillator seeded regenerative amplifier laser system. The amplifier laser system gives an output pulse energy of 2 mJ at 800 nm with a repetition rate of 1 kHz. The 800 nm laser beam was split into two portions. The larger portion of the 800 nm beam acted as the pump beam (for 800 nm excitation) or passed through a BBO crystal to generate the 400 nm pump beam by second harmonic generation (for 400 nm excitation). A small portion of the 800 nm beam was used to generate a white light continuum. The white light beam was split into two portions: one as the probe and another as the reference to correct the pulse-to-pulse intensity fluctuations. The pump beam was focused onto the sample with a beam size of 300 μm in diameter and overlapped with the smaller probe beam (100 μm in diameter). The time delay between the pump and probe pulses

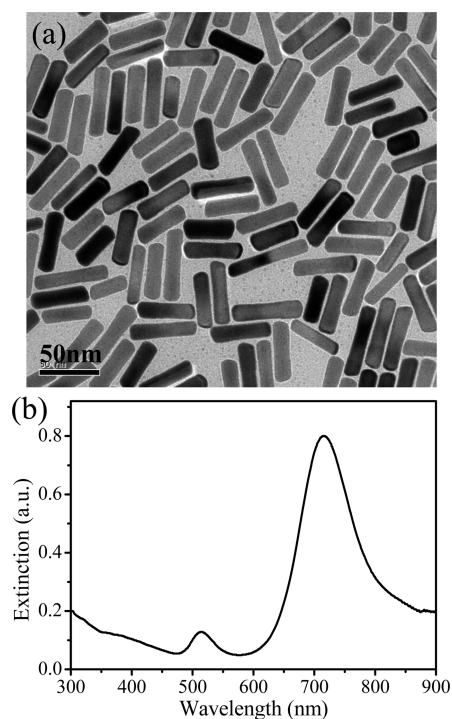


Figure 1. (a) TEM image and (b) extinction spectrum of the gold nanorod solution.

was varied by using a computer-controlled translation stage (Newport, ESP 300). All the time-resolved experiments were performed at room temperature. The aqueous nanoparticle suspensions were contained in a 1 mm path length cuvette. During the measurements, the pump and probe energies were kept low to minimize the photodamage to the samples. The extinction spectra of the sample before and after the experiments were checked and only subtle difference was observed, which suggests that the sample is stable and there is little sample damage during the whole experiments.

RESULTS AND DISCUSSIONS

Figure 1a shows the TEM image of gold nanorods with an average aspect ratio of 3.1. The average width and length were determined to be 14 and 44 nm, respectively. The corresponding UV–vis extinction spectrum is shown in Figure 1b. The two extinction bands at 515 and 715 nm correspond to the transverse and longitudinal plasmon modes of gold nanorods, respectively. The bandwidth of the longitudinal band is quite narrow (with full width at half-maximum of ~ 100 nm) and its amplitude is much larger than that of the transverse mode at 515 nm, indicating that the gold nanorods are of high quality with little impurity of spherical particles.

Figure 2a shows the transient absorption spectra in the spectral range from 450 to 800 nm at a delay time of 1.0 ps under different excitation fluences at 800 nm. It can be seen that the transient spectra are dominated by the transient bleaching of the longitudinal band with maximum at 705 nm, with transient absorption in the wings of the band. The bleaching of the transverse mode is overwhelmed by the transient absorption of wings of the longitudinal mode and only showed up as a small downward peak. As the energy of the 800 nm pump photon is less than

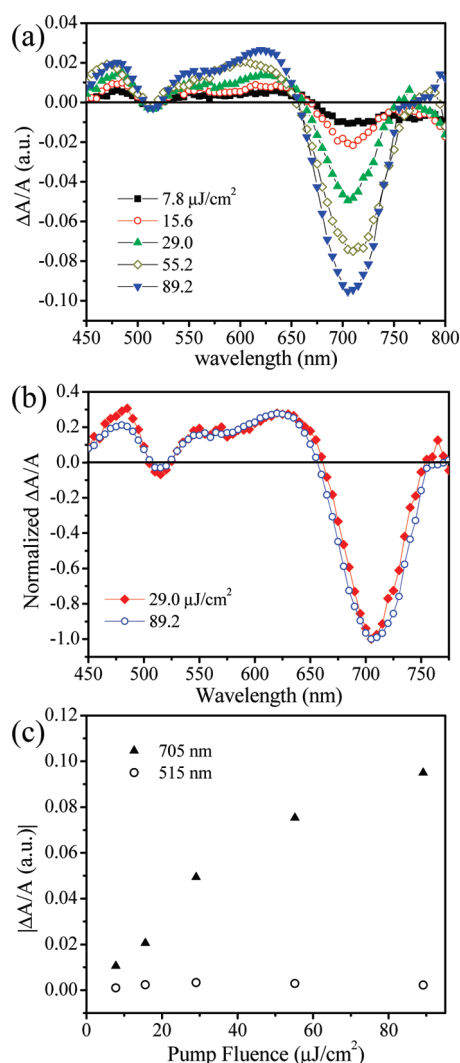


Figure 2. (a) Excitation fluence dependent transient absorption spectra of gold nanorods at a delay time of 1 ps under excitation at 800 nm. (b) Scaled transient absorption spectra (normalized the longitudinal bleaching amplitude to 1) under representative low (29.0 $\mu\text{J}/\text{cm}^2$) and high (89.2 $\mu\text{J}/\text{cm}^2$) excitation fluences. (c) Excitation fluence dependent amplitude of longitudinal mode and transverse mode.

the interband transition and the transverse mode, only the longitudinal mode is selectively excited directly. The excitation at 800 nm will result in heating of the electrons within the conduction band. The increase in the electronic temperature will lead to broadening of both the transverse and longitudinal bands and thus bleaching of both plasmon bands.

The overall shape of the transient spectra was found not very sensitive to the excitation fluence (Figure 2a,b). As the excitation fluence increases, the amplitude of the longitudinal band increases significantly, while the amplitude of the transverse band remains nearly constant. The width of the longitudinal band was also found to be slightly broadened under higher excitation fluences (Figure 2a,b). The band broadening can be ascribed to a faster dephasing of the coherent plasmon oscillation at higher electronic temperatures.^{35,36} Figure 2c plots the excitation fluence dependent bleaching amplitude of the longitudinal band (at 705 nm) and transverse band (at 515 nm). The bleaching amplitude of the longitudinal band was found to increase linearly

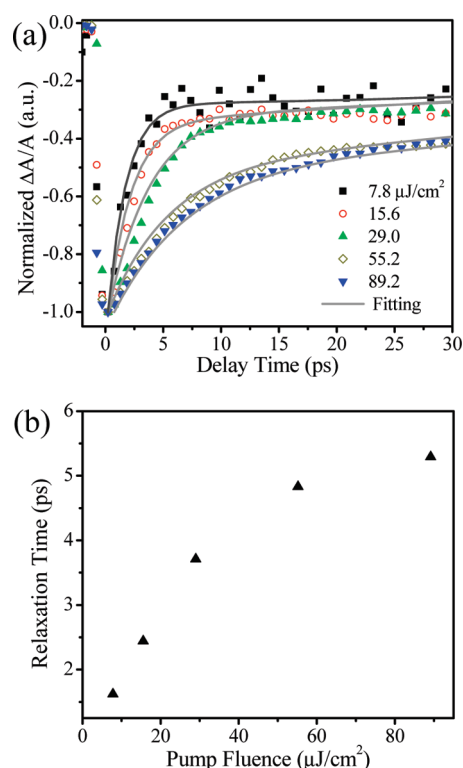


Figure 3. (a) Excitation fluence dependent bleaching dynamics of the longitudinal band at 705 nm under excitation at 800 nm. (b) Excitation fluence dependent electron–phonon coupling relaxation time constant at 705 nm.

with the excitation fluence at low excitation fluences and became saturated at higher excitation fluences (Figure 2c). A further increase in excitation fluence will cause the damage of the sample. The longitudinal band bleaching is much larger than that of the transverse band under excitation at 800 nm. The lack of excitation fluence dependence of the signal at 515 nm can be explained as due to two opposite effects: the increase of the positive dA/A (the wings of the transient absorption of the longitudinal band) and increase of the negative dA/A (bleaching of the transverse mode) nearly cancel out each other at ~ 515 nm.

Figure 3a shows the decay profiles of the longitudinal bleaching signals at 705 nm under different excitation fluences at 800 nm. The fast decay component is due to electron–phonon relaxation. The slow decay component corresponds to phonon–phonon relaxation, which is on a time scale of a few hundred picoseconds, consistent with the previously reported results for gold nanorods.²⁵ The excitation fluence dependent electron–phonon relaxation times are plotted in Figure 3b, which are obtained by fitting the decay profiles (0–30 ps) with a mono-exponential function

$$S(t) = A_L \exp(-t/\tau_{e-ph}^L) + A_0 \quad (1)$$

where τ_{e-ph}^L is the electron–phonon coupling relaxation time of longitudinal plasmon mode. The second term in eq 1 represents the slow phonon–phonon relaxation, which is assumed to be constant in the time window studied (1–30 ps). A_0 and A_L are the proportionality constants. The electron–phonon relaxation time increases linearly as the excitation fluence increases in the low perturbation regime. However, the electron–phonon

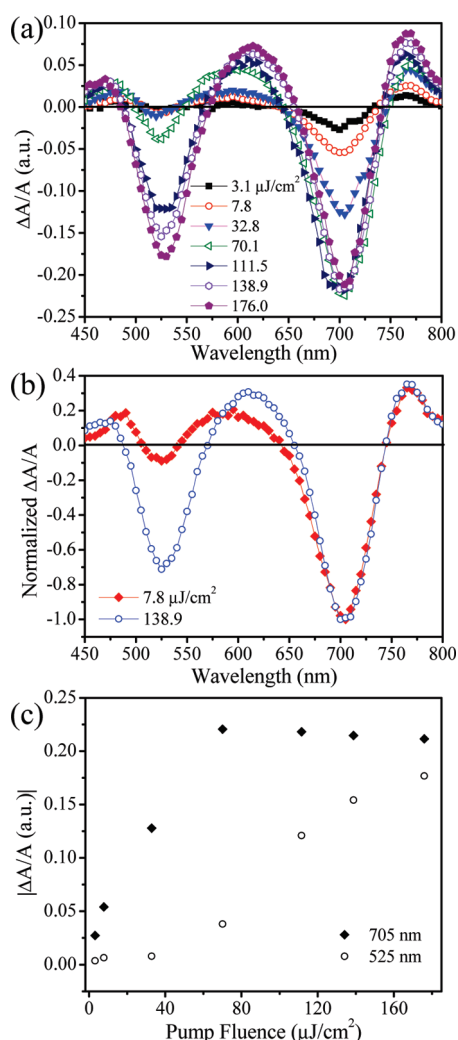


Figure 4. (a) Excitation fluence dependent transient absorption spectra of the gold nanorods solution under excitation at 400 nm at a delay time of 1 ps. (b) Scaled transient absorption spectra (normalized the longitudinal bleaching amplitude to 1) under representative low (7.8 $\mu\text{J}/\text{cm}^2$) and high (138.9 $\mu\text{J}/\text{cm}^2$) excitation fluences. (c) Excitation fluence dependent bleaching amplitudes at 705 nm (corresponding to longitudinal mode) and 525 nm (corresponding to the transverse mode).

relaxation time significantly deviates from the linear behavior at relatively high excitation fluences. These saturation behaviors are consistent with the results reported by Park et al.²⁵ They explained the linear relationship between the excitation fluence and the relaxation time scale as due to the temperature-independent electron heat capacity under low excitation fluences. As the excitation fluence increases, the electronic temperature increases. The electron heat capacity becomes dependent on the electronic temperature, which is responsible for the observed deviation from the linear relationship between the relaxation time scales and the excitation fluences. Comparison of Figures 2c and 3b indicates a good correlation between the signal amplitudes and electron–phonon time constants: both start to become saturated at excitation fluences of $\sim 40 \mu\text{J}/\text{cm}^2$. Both the excitation fluence dependent signal bleaching amplitude and electron–phonon relaxation time scales could be explained by the electronic temperature dependent electron heat capacity in the similar manner. The y-intercept of the linear fits in the lower

pump fluences could be taken as the electron–phonon coupling time constants. A time constant of 0.88 ps is determined for the longitudinal mode, which is slightly longer than the previously reported time constants of from 0.61 to 0.81 ps.^{29,34,37}

Figure 4a shows the transient absorption spectra of gold nanorods at a delay time of 1.0 ps under different excitation fluences at 400 nm. Excitation with 400 nm pulses can promote interband transitions from the d band into the s–p band above the Fermi level. The generated d-band holes recombine with the electrons from the conduction band within just a few tens of femtoseconds.³⁸ The absorbed energy is quickly transferred to the conduction electrons. Both the transverse and longitudinal bands are then simultaneously excited. The transient absorption spectra can be explained as spectral broadening of both longitudinal and transverse bands at a raised electronic temperature. The transient spectra under excitation at 400 nm show interesting excitation fluence dependent evolution (Figure 4a,b), strikingly different from that under excitation at 800 nm (Figure 2a, b). At low excitation fluences, the transient spectra are similar to those under excitation at 800 nm: the bleaching of the longitudinal band is much larger than the amplitude of the transverse bleaching band. As the excitation fluence increases, the amplitude of the longitudinal band bleaching steadily increases and becomes saturated and even decreases as the excitation fluence exceeds $\sim 70 \mu\text{J}/\text{cm}^2$ (Figure 4c). In contrast, the amplitude of the transverse mode only increases slightly at low excitation fluences until the excitation fluence reaches $\sim 70 \mu\text{J}/\text{cm}^2$ and then increases rapidly. At high excitation fluences, the amplitude of the transverse mode even becomes comparable to that of the longitudinal band (Figure 4).

Figure 5a,b show the decay profiles of the longitudinal and transverse bleaching signals at 705 and 525 nm, respectively. The fast decay is due to electron–phonon relaxation and the slow decay is due to phonon–phonon scattering. The excitation fluence dependent electron–phonon relaxation time scales for longitudinal and transverse bleaching signals are plotted in Figure 5c. The relaxation times of the longitudinal band were obtained by fitting the decay profiles using eq 1. Considering the signal at 525 nm is a superposition of the bleaching of transverse mode and transient absorption of the longitudinal mode, the decay signals at 525 nm were fitted by using

$$S(t) = A_L \exp(-t/\tau_{e-ph}^L) + A_T \exp(-t/\tau_{e-ph}^T) + A_0 \quad (2)$$

where the first term is related to induced absorption by the longitudinal mode and the relaxation time constant τ_{e-ph}^L was determined from fitting the longitudinal decay signal at 705 nm and kept fixed in the fitting. The second term is the decay of the transverse mode, and the decay constant is represented by τ_{e-ph}^T . The third term represents the slow phonon–phonon scattering process, which is assumed to be very slow in the time window studied (1–30 ps). A_L , A_T , and A_0 are the corresponding amplitudes. The electron–phonon relaxation times of the longitudinal mode vary from 2 to 6 ps. It is interesting to note that they have saturation behavior similar to that of their amplitudes; i.e., both the amplitude and relaxation time scale saturate and then start to decrease when the excitation fluence increases above $\sim 70 \mu\text{J}/\text{cm}^2$. These results could also be explained as electronic temperature independent heat capacity of electron gas at low excitation fluences (thus low electronic temperatures) and electronic temperature dependent heat capacity of electron gas at high excitation fluences (thus high electronic temperatures).²⁵

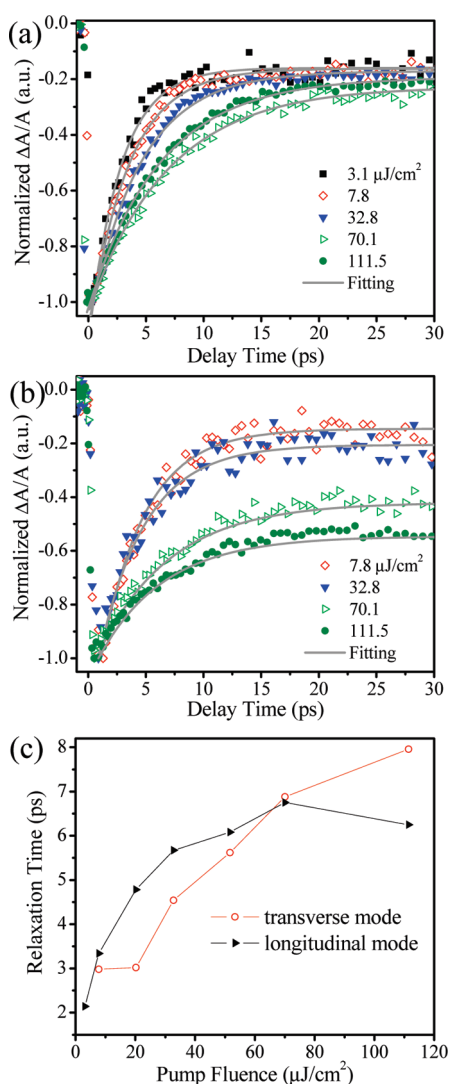


Figure 5. Excitation fluence dependent decay profiles of (a) longitudinal mode (at 705 nm) and (b) transverse mode (at 525 nm) under excitation at 400 nm. The solid lines are the fitting results. (c) Bleaching relaxation times of transverse and longitudinal bands as a function of excitation fluence.

At low excitation fluences below $\sim 70 \mu\text{J}/\text{cm}^2$, the relaxation time of longitudinal mode is similar (slightly longer) to that of the transverse mode, which is consistent with the previous observation by Park et al.²⁵ However, our results indicated that the transverse mode has longer electron phonon relaxation times than that of the longitudinal modes when the excitation fluence is above $\sim 70 \mu\text{J}/\text{cm}^2$.

So far there are very few reports on transient absorption studies on gold nanorods under excitation at 400 nm. Link et al. previously reported femtosecond electron dynamics of gold nanorods and found both transverse and longitudinal plasmon bands bleach after excitation at 400 nm.³³ They found that the transient bleaching of the transverse and longitudinal plasmon absorptions are of comparable intensities, although the longitudinal absorption was much larger than the transverse absorption in the steady state spectra. They ascribed the amplitude inconsistency between the transient and steady state spectra as a result of photoinstability of gold nanorods and a smaller effect of laser heating of the

electron gas on the transient broadening of longitudinal plasmon resonance. It was also noted that their gold nanorod samples had quite some impurity of spherical gold nanoparticles. They have also observed that there is no difference in the relaxation times measured at the transverse and longitudinal bleaching bands.

Here we used gold nanorods with high quality with little impurity of spherical gold nanoparticles. We have checked the extinction spectra of the samples before and after the measurements and only a very subtle difference ($<5\%$) in the extinction spectra was observed, which suggests that the samples were stable during the transient absorption and pump probe measurements. In our results, the bleaching of the longitudinal band is the dominant contribution at low excitation fluences at 400 nm. The amplitude of the bleaching of transverse band becomes comparable to that of the longitudinal band only at high excitation fluences when the longitudinal bleaching becomes saturated. These observations suggest that different amplitudes of longitudinal and transverse bleaching is not due to a smaller effect of laser heating of the electron gas on the transient broadening of longitudinal plasmon resonance. Under low excitation fluences at 400 nm, the absorbed energy is distributed into two modes according to their weights in the steady state extinction spectra. The longitudinal bleaching is thus dominant under low excitation fluences. When the longitudinal mode bleaching is saturated, the absorbed energy will mainly flow to the transverse mode, which causes the rapid increase in the bleaching of the transverse band. Another reason might be due to the small overlap between the excitation wavelength (400 nm) and the tail of the transverse mode. The transverse mode could further absorb the energy and contribute to the bleaching when the interband transition and longitudinal mode bleaching become saturated at high excitation fluences. The relaxation time of the transverse mode is slightly shorter than that of the longitudinal mode at low excitation fluences. However, the relaxation time of the transverse band increases rapidly as the excitation fluence increases. The fact that the transverse relaxation time becomes longer than that of the longitudinal band at excitation fluences above $\sim 70 \mu\text{J}/\text{cm}^2$ suggest that the electronic temperature further increases when more input energy is absorbed by the transverse mode. The bleaching of the transverse mode saturates at higher excitation fluences compared to the bleaching of the longitudinal mode, which is consistent with the smaller extinction coefficient of the transverse mode compared to that of the longitudinal mode.

In a related previous report by Jiang et al. on the polarization dependent transient absorption studies on gold nanorods under excitation at 800 nm, they found that the relaxation time probed in the perpendicular direction is always shorter than that probed in the parallel direction. They explained this polarization dependence as due to different weights of pump energy heating the anisotropy of gold nanorods.³⁴ In our studies, the electron-phonon relaxation time constants have strong correlation with the bleaching amplitude, which is directly related with the amount of the redistributed energies. With more energies are absorbed by the transverse mode, the increase of the bleaching signal of transverse mode is accompanied by a slower damping rate at raised electronic temperatures.

The transient absorption spectra show interesting dependence on the excitation wavelength. Excitation at 400 and 800 nm will lead to different distribution of energies into the transverse and longitudinal modes. Even though the bleaching of longitudinal and transverse modes was observed for both excitation wavelengths, the underlying broadening and bleaching mechanisms

are different. Excitation at 400 nm will excite both the transverse and longitudinal modes simultaneously. Both the broadening and bleaching were observed under all excitation fluences. However, longitudinal and transverse modes have the different effective absorption efficiencies. The longitudinal mode takes the dominant contribution in absorbing the energy and gives the dominant bleaching signals under the low excitation fluences. As the longitudinal mode becomes saturated upon a further increase of excitation energies, further increased input energies mainly flow to the transverse mode, consequently both the bleaching amplitude and electron–phonon relaxation time of transverse mode increase rapidly. It needs to be noted that 400 nm mainly excites the interband transitions at low excitation fluences. The absorbed energy by interband transition is quickly transferred to the conduction electrons within a few tens of femtoseconds, which then excite the transverse and longitudinal bands simultaneously.³⁸ This initial fast dynamical process cannot be accurately time-resolved in our experiments with limited resolution of ~ 100 fs. The situation under excitation at 800 nm is different. The photon energy of 800 nm is not sufficient to directly excite the transverse band, nearly all of the input energies are first absorbed by the longitudinal mode, which results in an increase in electronic temperature and consequent broadening and bleaching of both longitudinal and transverse bands. The transverse mode was excited indirectly in this case. The transient spectra are similar to those under excitation at 400 nm at low fluences. Further increasing the excitation energies does not cause further increase in the transverse mode bleaching because the transverse mode does not absorb energy directly, although the longitudinal bleaching band starts to become saturated.

CONCLUSIONS

In this work, we have presented a systematic study on electron dynamics of gold nanorods using excitation wavelength and fluence dependent femtosecond transient absorption and pump probe experiments. Using 400 and 800 nm laser pulses as the excitation sources, transverse and longitudinal modes can be selectively excited. The spectral characteristics of the transient absorption have been shown to be strongly dependent on the excitation wavelength and fluences. Laser pulses of 800 nm excite the longitudinal mode directly, which causes an increase in the electronic temperatures and subsequent broadening and bleaching of both the longitudinal and transverse modes. The transverse mode is thus excited indirectly. Pulses of 400 nm excite both the transverse and longitudinal modes simultaneously. At low excitation fluences, the energy is distributed into two modes according to their steady state extinction coefficients. The transient spectra are similar to those under excitation at 800 nm. However, as the excitation fluence exceeds a threshold, the bleaching of the longitudinal plasmon band saturates and the input energies mainly flow to the transverse mode. As a result, the bleaching of the transverse mode increases rapidly. The electron–phonon dynamics show a strong correlation with the bleaching amplitudes. Both the electron–phonon relaxation times and signal amplitudes show a linear dependence on the excitation fluences at low excitation fluences and significantly deviate from the linear dependence at higher excitation fluences. These results could be explained with a consistent picture: the bleaching amplitude and electron–phonon relaxation time are directly related to energy distribution into different modes, which are excitation wavelength and fluence dependent. Our studies help to

clarify the seemingly inconsistent results in the previous studies by different research groups and provide a consistent understanding of the electron dynamics of gold nanorods.

AUTHOR INFORMATION

Corresponding Author

*E-mail: chmxqh@nus.edu.sg.

ACKNOWLEDGMENT

We thank the financial support from the Faculty of Science, National University of Singapore (R-143-000-341-112) and DSTA Singapore (R-143-000-432-422).

REFERENCES

- (1) Barnes, W. L.; Dereux, A.; Ebbesen, T. W. *Nature* **2003**, *424*, 824.
- (2) Lal, S.; Link, S.; Halas, N. J. *Nat. Photonics* **2007**, *1*, 641.
- (3) Pelton, M.; Aizpurua, J.; Bryant, G. *Laser Photon. Rev.* **2008**, *2*, 136.
- (4) Gramotnev, D. K.; Bozhevolnyi, S. I. *Nat. Photonics* **2010**, *4*, 83.
- (5) Schuller, J. A.; Barnard, E. S.; Cai, W. S.; Jun, Y. C.; White, J. S.; Brongersma, M. L. *Nat. Mater.* **2010**, *9*, 193.
- (6) Bozhevolnyi, S. I. *Plasmonic Nanoguides and Circuits*; World Scientific Publishers: Singapore; Pan Stanford; Hackensack, NJ, 2009.
- (7) Kelly, K. L.; Coronado, E.; Zhao, L. L.; Schatz, G. C. *J. Phys. Chem. B* **2003**, *107*, 668.
- (8) Sun, Y. G.; Xia, Y. N. *Science* **2002**, *298*, 2176.
- (9) Murphy, C. J.; San, T. K.; Gole, A. M.; Orendorff, C. J.; Gao, J. X.; Gou, L.; Hunyadi, S. E.; Li, T. *J. Phys. Chem. B* **2005**, *109*, 13857.
- (10) Nikoobakht, B.; El-Sayed, M. A. *Chem. Mater.* **2003**, *15*, 1957.
- (11) Shankar, S. S.; Rai, A.; Ankamwar, B.; Singh, A.; Ahmad, A.; Sastry, M. *Nat. Mater.* **2004**, *3*, 482.
- (12) Jin, R. C.; Cao, Y. C.; Hao, E. C.; Metraux, G. S.; Schatz, G. C.; Mirkin, C. A. *Nature* **2003**, *425*, 487.
- (13) Jain, P. K.; Huang, X. H.; El-Sayed, I. H.; El-Sayed, M. A. *Acc. Chem. Res.* **2008**, *41*, 1578.
- (14) Durr, N. J.; Larson, T.; Smith, D. K.; Korgel, B. A.; Sokolov, K.; Ben-Yakar, A. *Nano Lett.* **2007**, *7*, 941.
- (15) Huang, X. H.; Neretina, S.; El-Sayed, M. A. *Adv. Mater.* **2009**, *21*, 4880.
- (16) Sonnichsen, C.; Franzl, T.; Wilk, T.; von Plessen, G.; Feldmann, J.; Wilson, O.; Mulvaney, P. *Phys. Rev. Lett.* **2002**, *88*, 077402.
- (17) Hu, M.; Hillyard, P.; Hartland, G. V.; Kosel, T.; Perez-Juste, J.; Mulvaney, P. *Nano Lett.* **2004**, *4*, 2493.
- (18) Zijlstra, P.; Chon, J. W. M.; Gu, M. *Nature* **2009**, *459*, 410.
- (19) Yu, Y. Y.; Chang, S. S.; Lee, C. L.; Wang, C. R. C. *J. Phys. Chem. B* **1997**, *101*, 6661.
- (20) Rosei, R. *Phys. Rev. B* **1974**, *10*, 474.
- (21) Rosei, R.; Culp, C. H.; Weaver, J. H. *Phys. Rev. B* **1974**, *10*, 484.
- (22) Bigot, J. Y.; Halte, V.; Merle, J. C.; Daunois, A. *Chem. Phys.* **2000**, *251*, 181.
- (23) Voisin, C.; Del Fatti, N.; Christofilos, D.; Vallee, F. *J. Phys. Chem. B* **2001**, *105*, 2264.
- (24) Perner, M.; Bost, P.; Lemmer, U.; von Plessen, G.; Feldmann, J.; Becker, U.; Mennig, M.; Schmitt, M.; Schmidt, H. *Phys. Rev. Lett.* **1997**, *78*, 2192.
- (25) Park, S.; Pelton, M.; Liu, M.; Guyot-Sionnest, P.; Scherer, N. F. *J. Phys. Chem. C* **2007**, *111*, 116.
- (26) Del Fatti, N.; Voisin, C.; Achermann, M.; Tzortzakakis, S.; Christofilos, D.; Vallee, F. *Phys. Rev. B* **2000**, *61*, 16956.
- (27) Link, S.; Burda, C.; Mohamed, M. B.; Nikoobakht, B.; El-Sayed, M. A. *Phys. Rev. B* **2000**, *61*, 6086.
- (28) Groeneveld, R. H. M.; Sprik, R.; Lagendijk, A. *Phys. Rev. B* **1995**, *51*, 11433.
- (29) Link, S.; El-Sayed, M. A. *J. Phys. Chem. B* **1999**, *103*, 8410.

- (30) Inouye, H.; Tanaka, K.; Tanahashi, I.; Hirao, K. *Phys. Rev. B* **1998**, *57*, 11334.
- (31) Arbouet, A.; Voisin, C.; Christofilos, D.; Langot, P.; Del Fatti, N.; Vallee, F.; Lerme, J.; Celep, G.; Cottancin, E.; Gaudry, M.; Pellarin, M.; Broyer, M.; Maillard, M.; Pileni, M. P.; Treguer, M. *Phys. Rev. Lett.* **2003**, *90*, 177401.
- (32) Guillet, Y.; Charron, E.; Palpant, B. *Phys. Rev. B* **2009**, *79*, 195432.
- (33) Link, S.; Burda, C.; Mohamed, M. B.; Nikoobakht, B.; El-Sayed, M. A. *Phys. Rev. B* **2000**, *61*, 6086.
- (34) Jiang, Y.; Wang, H. Y.; Xie, L. P.; Gao, I. R.; Wang, L.; Zhang, X. L.; Chen, Q. D.; Yang, H.; Song, H. W.; Sun, H. B. *J. Phys. Chem. C* **2010**, *114*, 2913.
- (35) Kruglyak, V. V.; Hicken, R. J.; Matousek, P.; Towrie, M. *Phys. Rev. B* **2007**, *75*, 035410.
- (36) Schoenlein, R. W.; Lin, W. Z.; Fujimoto, J. G.; Eesley, G. L. *Phys. Rev. Lett.* **1987**, *58*, 1680.
- (37) Hodak, J. H.; Martini, I.; Hartland, G. V. *J. Phys. Chem. B* **1998**, *102*, 6958.
- (38) Del Fatti, N.; Vallee, F. *Appl. Phys. B: Laser Opt.* **2001**, *73*, 383.